

# DEVELOPMENT OF HIGH TEMPERATURE AND HIGH STRAIN RATE SUPER PLASTIC DEEP DRAWING PROCESS FOR 5656 AL ALLOY CYLINDRICAL CUPS

CHENNAKESAVA R ALAVALA

Department of Mechanical Engineering, JNT University, Hyderabad, India

E-mail: chennakesava@jntuh.ac.in

**Abstract-** Recent demands of world trade and automobile production are for the reduction of manufacturing lead time and weight reduction. The present work emphasizes the formability of cylindrical cups using high temperature-high strain rate (HTHSR) superplastic forming process. A statistical approach based on Taguchi Techniques and finite element analysis were adopted to determine the formability of 5656 Al alloy cups. The process parameters were temperature, strain rate, coefficient of friction and blank holder velocity. The FEA results obtained using finite element software namely D-FORM were authenticated through the experimental results. For 5656 Al alloy, the HTHSR superplastic forming process has happened at strain rate of  $1.0 \text{ s}^{-1}$  and temperature of  $400^\circ\text{C}$ .

**Keywords-** 5656 Al alloy, high temperature, high strain rate, superplastic deep drawing process, coefficient of friction, cylindrical cups, forming limit diagram.

## I. INTRODUCTION

Deep drawing is large deformation elasto-plastic process for shaping flat sheets into cup-shaped products without fracture or excessive localized thinning. Products include automotive parts, aircraft frames, submarine hulls, beverage cans and domestic appliances. As the sheet material is drawn radially inwards the flange experiences radial tension, circumferential compression. Radial tensile stress in the flange is produced on the cup wall induced by the punch force. For larger draw ratios of deep drawn cups, higher tensile stress is required on the cup walls [1]. One of the major defects that occur in deep drawing operations is the wrinkling of sheet in the flange region of the cup. The radial drawing stress and tangential compressive stress are responsible for the formation of wrinkles. Blank holder is employed to suppress the wrinkle formation. Due to applied force on the blank holder, stress normal to the thickness increases which detains any formation of wrinkles. But, the large force on the blank holder can cause fracture at the cup wall and punch profile. In order to overcome this difficulty, movable blank holder is introduced in the present work. In metal forming processes, the friction effects the strain distribution at tool blank interface and drawability of sheet metal. In an experimental work carried out on the warm deep drawing process of the EDD steel, the thinning at punch corner radius is found to be lesser at  $200^\circ\text{C}$  [2].

The conventional superplastic forming is carried out at low strain rates in the range of  $10^{-4} - 10^{-3} \text{ s}^{-1}$  and high temperatures above recrystallization. Several investigations have been carried out to boost the superplastic properties of aluminum alloys. Further, high temperature and high strain rate (HTHSR) superplastic forming process was developed to reduce

the forming time of several aluminum alloys such as AA1050 [4], AA2014 [5], AA2017 [6], AA2024 [7], AA2219 [9], AA2618 [9], AA3003 [10], AA5059 [11] and AA5051 [12]. For all these materials in the finite element simulations, a forming limit diagram (FLD) has been successfully applied to analyze the fracture phenomena by comparing the strain status.

Because of high strength and excellent formability 5056 aluminum alloy is used extensively in cold forming applications as well as wire forms and hinge pins. 5056 aluminum alloy also has excellent corrosion resistance and can be used in atmospheres such as salt water where corrosion would normally be a problem with other metals. The importance of the present work was to discover fitness of 5656 aluminum alloy for high temperature and high strain rate superplastic forming process. The investigation was concentrated on the process variables such as temperature, strain rate, coefficient of friction and blank holder velocity. The design of experiments was carried out using Taguchi technique and HTHSR superplastic deep drawing process was implemented using the finite element analysis software namely D-FORM 3D. The results acquired through the finite element analysis were endorsed experimentally.

## II. MATERIALS AND METHODS

5056 aluminum alloy consists of: Al (95.00%), Mg (5.00%), Mn ( $\leq 0.12\%$ ), Cr ( $\leq 0.12\%$ ), Si (0.30% max), Fe (0.40% max), Cu (0.10% max) and Zn (0.10% max). In the present work, 5656 aluminum alloy was used to fabricate cylindrical cups. The levels chosen for the controllable process variables are summarized in table 1. The orthogonal array (OA), L9 was selected to carry out experimental and finite element analysis (FEA). The assignment of variables in the OA matrix is given in table 2.

**Table 1: Process variables and levels**

Factor	Symbol	Level-1	Level-2	Level-3
Temperature, °C	A	300	400	500
Strain rate, 1/s	B	0.1	0.5	1.0
Coefficient of friction	C	0.10	0.15	0.20
BH velocity, mm/s	D	0.13	0.7	0.20

**Table 2: Orthogonal array (L9) and process variables**

Treat No.	A	B	C	D
1	1	1	1	1
2	1	2	2	2
3	1	3	3	3
4	2	1	2	3
5	2	2	3	1
6	2	3	1	2
7	3	1	3	2
8	3	2	1	3
9	3	3	2	1

### 2.1. Fabrication and Testing of Deep Drawn Cups

The sheets of 5656 Al alloy were cut to the required blank size as defined in [5]. The blank specimens were heated in a muffle furnace to the desired temperature as per the design of experiments. The blank force was calculated using Eq. (1). The cups were fabricated using hydraulically operated deep drawing machine.

$$\text{Drawing force, } F_d = \pi dt[D/d - 0.6]\sigma_y \quad (1)$$

$$\text{Clearance, } c = t \pm \mu\sqrt{10t} \quad (2)$$

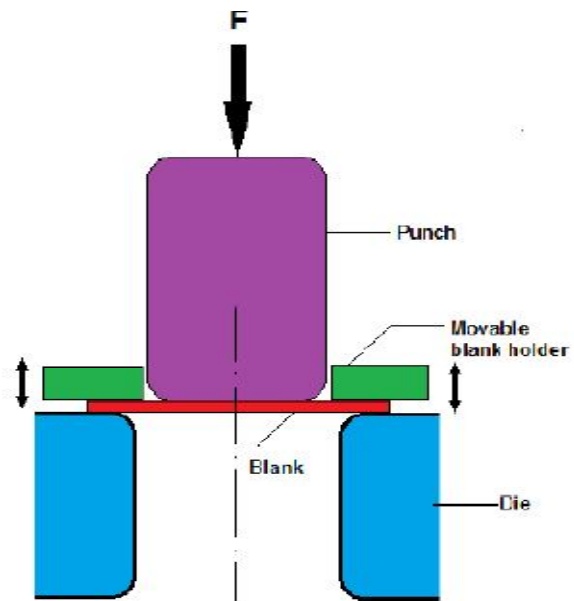
### 2.2. Finite Element Modeling and Analysis

The finite element modeling and analysis was carried using D-FORM 3D software. The cylindrical sheet blank was created with desired diameter and thickness using CAD tools. The cylindrical top punch, cylindrical bottom hollow die and movable blank holder were also modeled with appropriate inner and outer radius and corner radius using CAD tools. The clearance between the punch and die was calculated as in Eq. (2). The sheet blank was meshed with 14174 tetrahedral elements.

In the present work, moving blank die was used to hold the blank at a predefined speed different to the punch speed. The contact between blank/punch, blank/blank holder and die/blank were coupled as contact pair (Fig.1). The mechanical interaction between the contact surfaces was assumed to be frictional contact and modeled as Coulomb's friction model as defined in Eq. (3). The finite element analysis was chosen to find the metal flow, effective stress, height of the cup, and damage of the cup. The finite element analysis was carried out using D-

FORM 3D software according to the design of experiments. The Coulomb's friction model is given by

$$\tau_f = \mu p \quad (3)$$



### III. RESULTS AND DISCUSSION

In the present work, movable and non-deformable blank holder has been employed. This moves along with punch with different velocity.

**Table 3: ANOVA summary of the von Mises stress**

Source	Sum 1	Sum 2	Sum 3	SS	$\nu$	$V$	$P$
A	2533.68	1707.88	1583.56	177788.99	2	88894.49	14.49
B	2628.35	1573.19	1623.59	236161.14	2	118080.57	19.24
C	3006.96	1424.48	1393.68	567537.77	2	283768.88	46.25
D	2642.36	1572.17	1610.60	245700.35	2	122850.18	20.02
e				0.00	0		0.00
T	10811.34	6277.73	6211.43	1227188.24	8		100.00

**Note:**SS is the sum of square,  $\nu$  is the degrees of freedom,  $V$  is the variance,  $F$  is the Fisher's ratio,  $P$  is the percentage of contribution and  $T$  is the sum squares due to total variation.

### 3.1. Effect of Process Variables on von Mises Stress

The percent contributions of A, B, C and D vary in a large range between 14.49% and 46.25% towards variation in the von Mises stress (Table 3). The descending order of process variables is the coefficient of friction (C), the blank holder velocity (D), the strain rate (B) and the temperature (A). The coefficient of friction by itself has a major effect (46.25%) on the von Mises stress. The least contribution (14.49%) is of blank temperature to get variation in the von Mises stress. The strain rate (B) and blank holder (BH) velocity (D) have contributed,

respectively, 20.02% and 19.24% of variation in the von Mises stress.

Fig. 2 presents the von Mises stress induced in 5656 aluminum alloy during the cylindrical cup drawing process as a function of temperature and strain rate. The von Mises stress decreases with initial blank temperature from 300 to 500°C. It is also observed that the von Mises stress decreases with an increase in the strain rate from 0.1 to 1.0 s<sup>-1</sup>. Dynamic cooling takes during deep drawing process of 5056 aluminum alloy sheet material. The strain softening is the region in which the stress in the material is actually decreasing with an increase in strain. Strain hardening is a result of plastic deformation, a permanent change in shape to ensue cylindrical cup [13]. For the 5656 aluminum alloy, the strain hardening coefficient is the resultant of strain hardening mechanism depending on strain and softening mechanism depending on temperature [14].

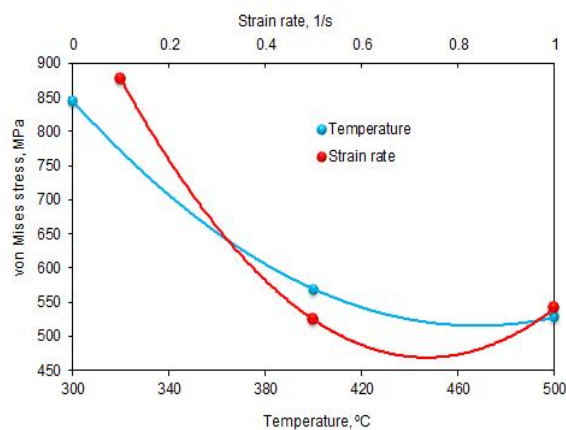


**Fig. 2. The von Mises stress as a function of temperature and strain rate.**

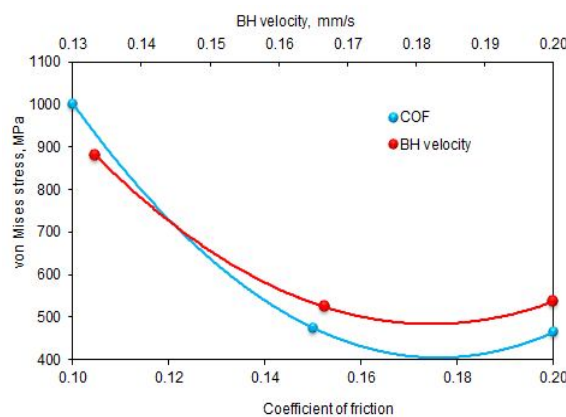


**Fig. 3. The von Mises stress as a function of COF and BH velocity.**

Fig.3 depicts the von Mises stress as a function of COF (coefficient of friction) and blank holder(BH) velocity. It is perceived that the von Mises stress decreases with increase of COE and BH velocity. In deep drawing process, friction initiates from sliding contact between the tool and the blank sheet. The surface asperities of the blank sheet undergo stretch

deformation on account of the tangential load along the sliding contact. Once the surface asperities become flattened due to stretch deformation, further increase of friction does not demand large drawing force and consequently fall in the von Mises stress. In the present work, the blank holder was allowed to move along the punch but at different velocities to avoid wrinkles in the cup. As the blank holding force was maintained constant in this work. The BH velocities were designed to avoid additional frictional force on the blank sheet and merely to avoid the formation of wrinkles in the flange area of the cup. As seen from Fig.3, the individual influences of OE and BH velocity are nearly the same.

The FEA results of von Mises stress as a function of von Mises strain are shown in Figs. 4 to 6 for various test conditions as per the design of experiments. For trials 1, 2 and 3, the temperature was 300°C and other process parameters were varied as mentioned in Tables 1 and 2. The maximum values of von Mises stresses for trails 1, 2 and 3 are, respectively, 1662.07, 426.13 and 445.47 MPa. For trial 1 all the process variables have level -1 values as stated in Table 2. As observed from Figs. 2 and 3, the von Mises stress is high for level-1 values of process variables. Consequently, the resultant von Mises stress is a gigantic value of 1662.07 MPa as shown in Fig.4. For trials 2 and 3, the process variables have values of level-2 and level-3, respectively, except the temperature which is at 300°C. The von Mises stresses for trails 2 and 3 are, respectively, 426.13 and 455.47 MPa. The slight increased values are also observed for von Mises stress at level-3 of process variables as seen from Figs. 2 and 3. For trials 4, 5 and 6, the temperature was 400°C and other process parameters were varied as mentioned in Tables 1 and 2. The maximum values of von Mises stresses for trails 4, 5 and 6 are, respectively, 515.40, 497.33 and 595.16 MPa. The von Mises stress values for trials 4 and 5 are nearly the same with very small deviation due to variation of levels pertaining to process variables.

The von Mises stress induced for trial 6 conditions is higher than those of trials 4 and 5. In case of trails 4 and 5, the cups are fractured without undergoing full plastic deformation. For trials 7, 8 and 9, the temperature was 500°C and other process parameters were varied as mentioned in Tables 1 and 2. The maximum values of von Mises stresses for trails 7, 8 and 9 are, respectively, 450.88, 649.73 and 482.96 MPa. Due to premature failure of the cups, the von Mises stress values for trials 7 and 9 are lower than that of trial 8. The applied load as a function of punch stroke is shown in Fig. 7. The sudden drop of punch load curve for trials 1, 2, 3, 4, 5, 7, and 9 are due to fracture of sheet blank without complete plastic deformation conferring to the design of experiments in the present work. However, the plastic deformation

is continued till the formation of cups for trials 6 and 8.

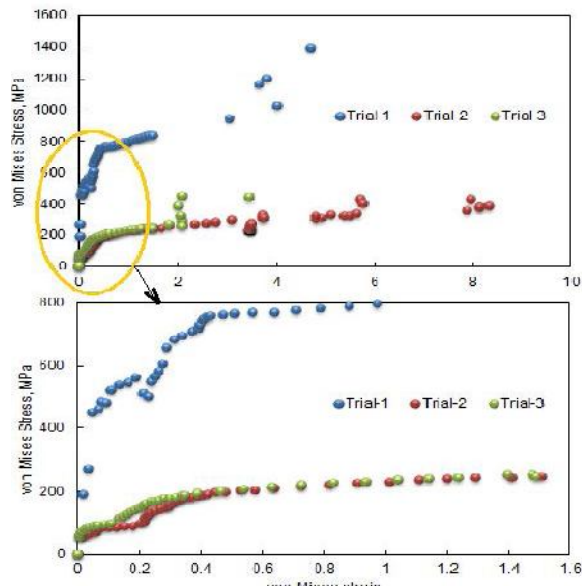


Fig. 4. Effect of process parameters on the von Mises stress for trials 1, 2 and 3.

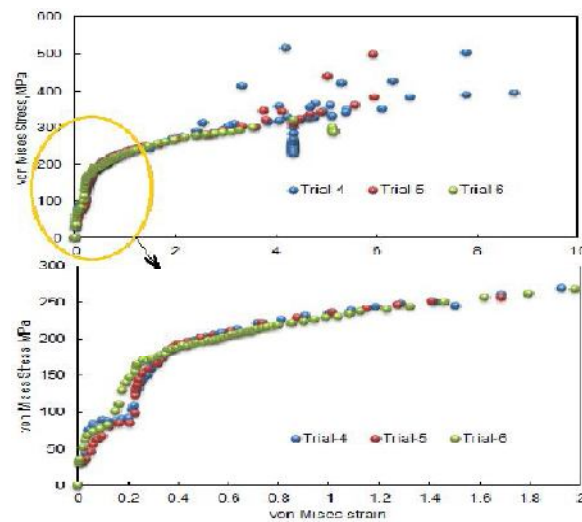


Fig.5. Effect of process parameters on the von Mises stress for trials 4, 5 and 6.

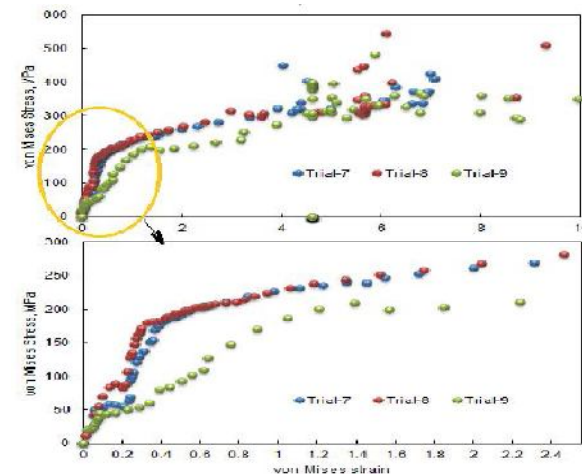


Fig.6. Effect of process parameters on the von Mises stress for trials 7, 8 and 9.

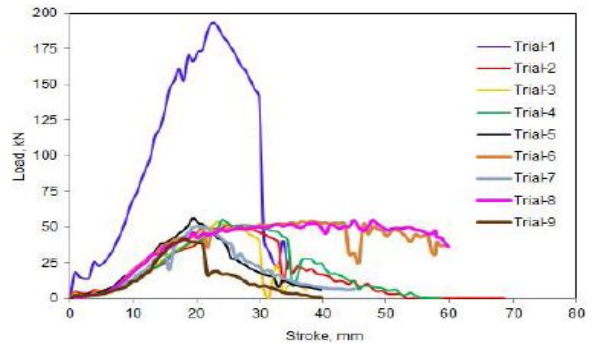


Fig. 7. Applied load as a function punch stroke.

Table 4: ANOVA summary of the surface expansion ratio

Source	Sum 1	Sum 2	Sum 3	SS	$\nu$	$F$	$P$
A	66.74	41.43	19.46	373.18616	2	186.59308	13.05
B	45.62	72.9	9.11	682.92696	2	341.46348	23.88
C	6.25	89.56	31.82	1214.2543	2	607.12714	42.47
D	5.12	73.73	33.32	483.01069	2	242.30534	16.96
e				103.87	0		0
T	123.73	279.62	93.91	2859.25	8		100.00

### 3.2 Effect of Process Variables on Surface Expansion Ratio

In the deep drawing process the plastic deformation in the surface is much more prominent than in the thickness of sheet. As per the ANOVA summary of surface expansion ratio given in Table 4., the temperature, (A), strain rate (B), coefficient of friction (C), and BH velocity (D) contribute, respectively, 13.05%, 23.88%, 42.47% and 16.96% respectively towards variation in the surface expansion ratio.

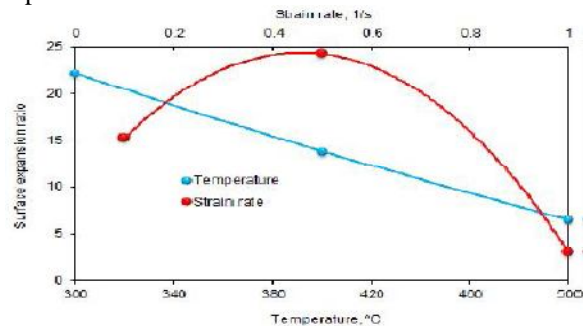
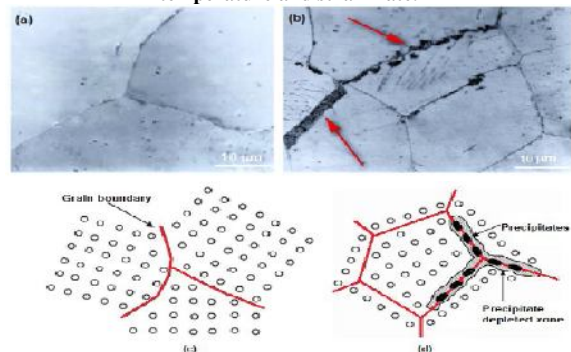
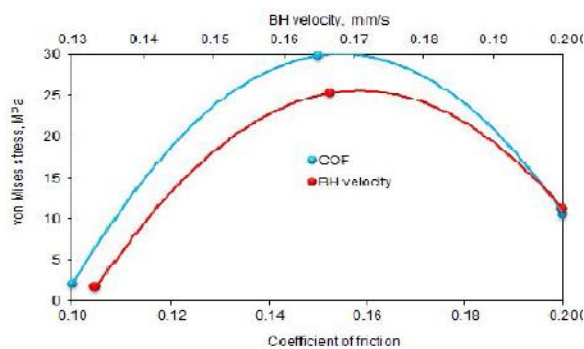


Fig. 8. The surface expansion ratio as a function of temperature and strain rate.



**Fig. 9. Microstructure of deep drawn 5056 Al alloy sheet: (a) heated to 300°C and (b) heated to 500°C, (c) schematic presentation of case (a) and schematic presentation of case (b).** The surface expansion ratio decreases with an increase in the operating blank temperature from 300°C to 500°C as shown in Fig.8. The reason is very unusual to understand. The operating temperature of 400°C and above may be consequence for fine recrystallization resulting low surface expansion ratio. The degree of recrystallization is dependent on thermo-mechanical processing conditions including temperature of the sheet blank. The sheet blank at initial high temperature cools very fast than those at low temperature. At high temperature, reprecipitation of soluble phases like Al<sub>2</sub>Cu and Mg<sub>2</sub>Si in a finer form are observed as shown in Fig. 9b of deep drawn sheet heated to 500°C. Fig.9a represents no reprecipitation in the deep drawn sheet heated to 300°C. Most grain boundaries (Fig.9c) are preferred sites for the precipitation of new phases (Fig.9d). The effect of strain rate on the surface expansion ratio is also shown in Fig.8. The surface expansion ratio increases initially due to strain softening for an increase in the strain rate from 0.1 to 0.5 s<sup>-1</sup> and later on it decreases owing to strain hardening for an increase in the strain rate from 0.5 to 1.0 s<sup>-1</sup>. High strain rate sensitivity is typically associated with a fine grain microstructure.

The surface expansion ratio is high for the COE of 0.15 due to stretch deformation as shown in Fig.10. The surface expansion ratio was increased with an increase in the blank holder velocity from 0.13 to 0.17 mm/s and later on it decreases for a change in blank holder velocity from 0.17 to 0.20 mm/s. At high velocities, the blank holder comes in contact with the blank early and accordingly, the material is restrained to flow into the die resulting reduction in the surface expansion. In contrast at low velocities, the blank holder comes in contact with the blank late and consequently, the material is not restrained to flow into the die resulting enhancing the surface expansion. The FEA results of surface expansion ratio are revealed in Fig.11 for various test conditions as per the design of experiments. For the best quality of cup, the surface expansion ratio should be in the range of 1.50 to 1.63.



**Fig. 10. The surface expansion ratio as a function of COF and BH velocity.**

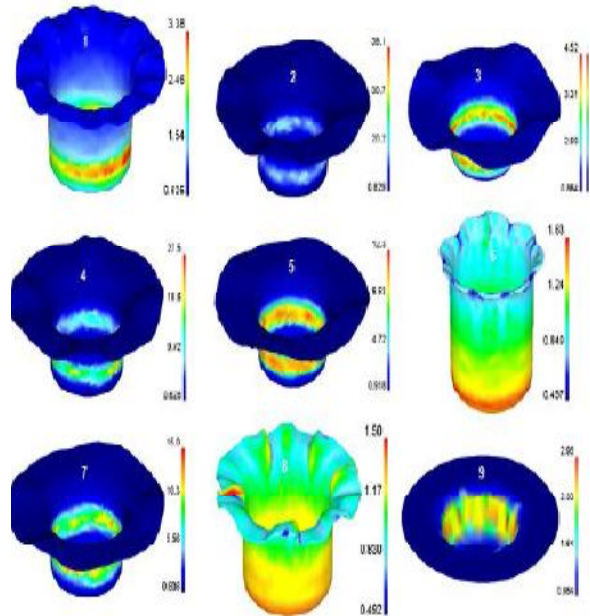


**Fig.11. Effect of process parameters on the surface expansion ratio.**

**3.3FLDs and Damages in the Cups**

Fig.12 depicts the forming limit diagram (FLD) with damages in the cylindrical cups drawn from 5656 aluminum alloy sheets at temperature 300°C. The FLD for the cylindrical cup drawn under trial 1 experiences pure shear and uniaxial tension. Initially, the sheet blank experiences pure shear till 40% of the desired cup is formed and later on the formation of cup is failed due to uniaxial tension experienced by the sheet blank. The FLD for the conical cup drawn under trial 2 and 3 experiences pure shear and equibiaxial tension. For trials 2 and 3, the sheet blanks has undergone pure shear till 61% and 45%, separately, of the desired cup is formed and later on the formation of cup is failed due to equibiaxial tension [15].

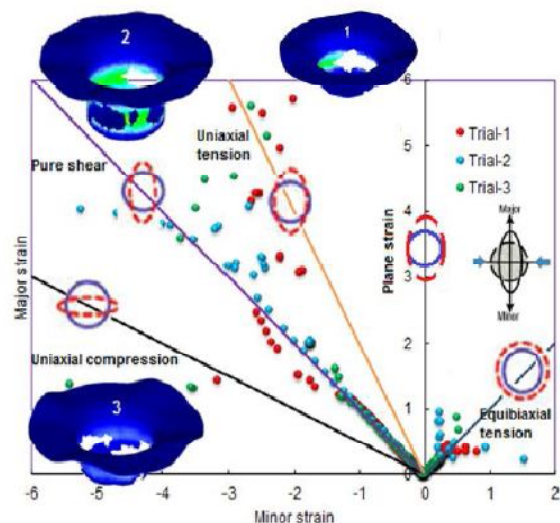


**Fig.12. Forming limit diagram with damage in the cups drawn at temperature 300°C.**

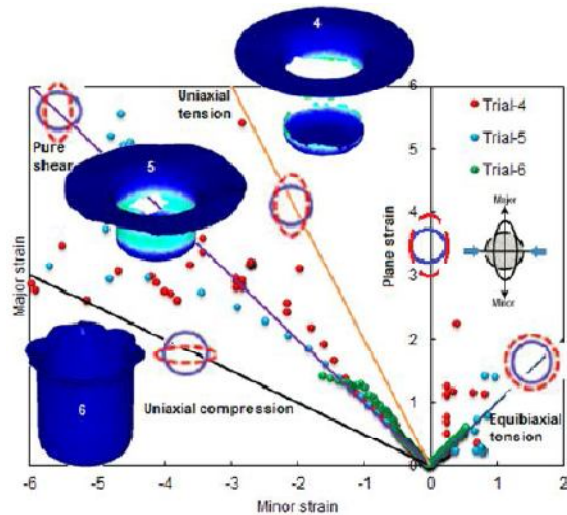


Fig. 13. Forming limit diagram with damage in the cups drawn at temperature 400°C.

Fig.13 illustrates the forming limit diagram and damages in the cups drawn from 5656 aluminum alloy sheets with trials, 4, 5 and 6 at temperature 400°C. Cups drawn on trials 4 and 5 have damaged due to high uniaxial tension and stretching. The percentages of cups formed for trials 4 and 5 are 62% and 56%, respectively. For trial 6, total cup is formed without rupture. Cups drawn from trial 7 is fractured owing to uniaxial tension as shown in Fig.14. The cup has reached 58% of the desired size of the cup. During the last stages of cup formation, the blank sheet between the blank holder and bottom die has experienced stretching as a result of equibiaxial tension achieving 69% of quality cup. Cup drawn with trial 9 conditions has obtain 36% of the final cup before it ruptures due to uniaxial tension.

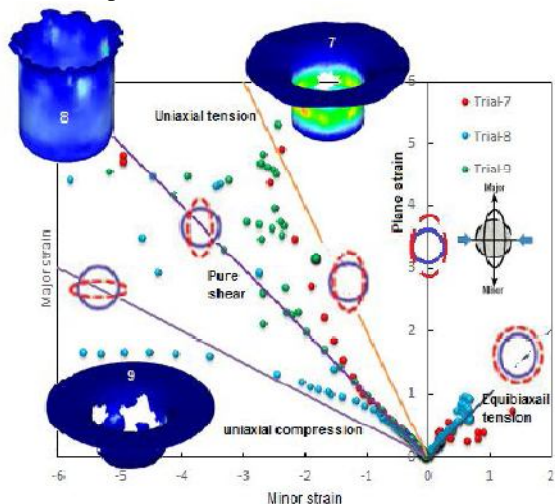


Fig. 14. Forming limit diagram with damage in the cups drawn at temperature 500°C.

In the present work, the critical value of the damage factor is defined as follows:

$$D_f = \int \frac{\sigma^*}{\sigma_{vm}} d\epsilon \quad (4)$$

where  $\sigma^*$  is the tensile maximum principal stress,  $\sigma_{vm}$  is the von Mises stress and  $d\epsilon$  is the effective strain

increment. Fracture takes place when the damage factor has reached its critical value. The damage factors for all the trials are illustrated in Fig.15. The least damage factor is associated with trail 6 of the design of experiments. Therefore, for the successful the optimum levels of the process variables are taken of trial 6 conditions from Tables 1 and 2. Experimentally deep drawn cup with test conditions of trial 6 is shown in Fig.16. The temperature and strain rate of trial 6 conditions are 400°C and 1.0 s<sup>-1</sup> which represent the high temperature and high strain rate superplastic forming process.

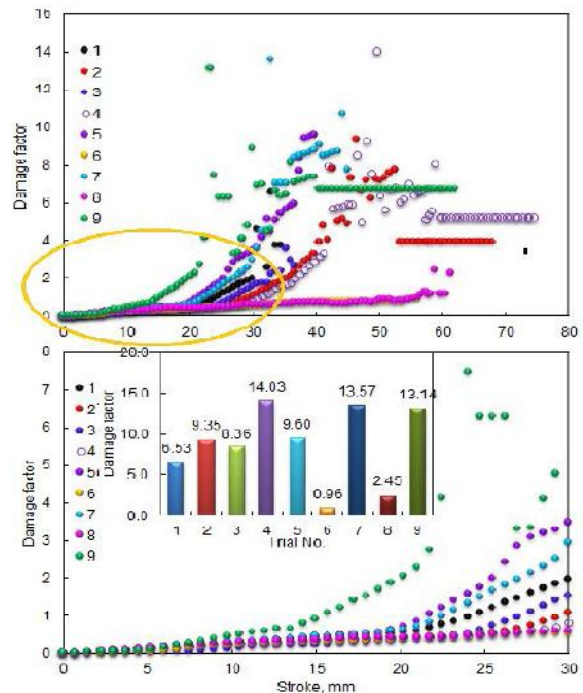


Fig. 15. Damage factors under different trials.



Fig. 16. Successful drawn from trial 6 conditions.

## CONCLUSIONS

In this paper, the circular cups of 5656 aluminum alloy sheet have been formed numerically and experimentally. The von Mises stress was least at

operating temperature of 500°C and strain rate of 1.0 s<sup>-1</sup>. The reasons for the failure of cups were due to uniaxial tension and stretching. 5656 aluminum alloy has been found to yield successful cup at high temperature-high strain rate (HTHSR) superplastic forming process. Trial 6 test conditions satisfy the successful execution of HTHSR superplastic forming process.

## REFERENCES

- [1] A. C. Reddy, Finite element analysis of reverse superplastic blow forming of Ti-Al-4V alloy for optimized control of thickness variation using ABAQUS, *Journal of Manufacturing Engineering*, vol.1, no.01, pp.06-09, 2006.
- [2] A. C. Reddy, T. Kishen Kumar Reddy and M. Vidya Sagar, Experimental characterization of warm deep drawing process for EDD steel, *International Journal of Multidisciplinary Research & Advances in Engineering*, vol.4, no.3, pp.53-62, 2012.
- [3] A. C. Reddy, Evaluation of local thinning during cup drawing of gas cylinder steel using isotropic criteria, *International Journal of Engineering and Materials Sciences*, vol.5, no.2, pp.71-76, 2012.
- [4] A. C. Reddy, Homogenization and Parametric Consequence of Warm Deep Drawing Process for 1050A Aluminum Alloy: Validation through FEA, *International Journal of Science and Research*, vol. 4, no. 4, pp.2034-2042, 2015.
- [5] A. C. Reddy, Parametric Optimization of Warm Deep Drawing Process of 2014T6 Aluminum Alloy Using FEA, *International Journal of Scientific & Engineering Research*, vol.6, no.5, pp.1016-1024, 2015.
- [6] A. C. Reddy, Finite Element Analysis of Warm Deep Drawing Process for 2017T4 Aluminum Alloy: Parametric Significance Using Taguchi Technique, *International Journal of Advanced Research*, vol.3, no.5, pp.1247-1255, 2015.
- [7] A. C. Reddy, Parametric Significance of Warm Drawing Process for 2024T4 Aluminum Alloy through FEA, *International Journal of Science and Research*, vol.4, no.5, pp.2345-2351, 2015.
- [8] A. C. Reddy, Formability of High Temperature and High Strain Rate Superplastic Deep Drawing Process for AA2219 Cylindrical Cups, *International Journal of Advanced Research*, vol.3, no.10, pp.1016-1024, 2015.
- [9] C.R. Alavala, High temperature and high strain rate superplastic deep drawing process for AA2618 alloy cylindrical cups, *International Journal of Scientific Engineering and Applied Science*, vol.2, no.2, pp.35-41, 2016.
- [10] C.R. Alavala, Practicability of High Temperature and High Strain Rate Superplastic Deep Drawing Process for AA3003 Alloy Cylindrical Cups, *International Journal of Engineering Inventions*, vol.5, no.3, pp.16-23, 2016.
- [11] C.R. Alavala, High temperature and high strain rate superplastic deep drawing process for AA5049 alloy cylindrical cups, *International Journal of Engineering Sciences & Research Technology*, vol.5, no.2, pp.261-268, 2016.
- [12] C.R. Alavala, Suitability of High Temperature and High Strain Rate Superplastic Deep Drawing Process for AA5052 Alloy, *International Journal of Engineering and Advanced Research Technology*, vol.2, no.3, pp.11-14, 2016.
- [13] A. Nader, Forming of Aluminum alloys at elevated temperatures-part1: Material characterization, *International Journal of Plasticity*, vol.22, pp.314-341, 2006.
- [14] W. S. Lee, G. W. Yeh, The plastic deformation behaviour of AISI 4340 alloy steel subjected to high temperature and high strain rate loading conditions, *Journal of materials processing technology*; vol.71, pp. 224–234, 1997.
- [15] L.C. Tsao, H.Y. Wu, J.C. Leong, C. J. Fang, Flow stress behaviour commercial pure titanium sheet during warm tensile deformation, *Materials and Design*, vol.34, pp.179–184, 2012.

★ ★ ★